The Origin of Soft X-rays in DQ Herculis

K. Mukai[1,2], M. Still[2]

Code 662, NASA/Goddard Space Flight Center, Greenbelt, MD 20771, USA.

and

F. A. Ringwald

Department of Physics, California State University, Fresno, 2345 E. San Ramon Ave., MS MH37, Fresno, CA 93740-8031, USA.

ABSTRACT

DQ Herculis (Nova Herculis 1934) is a deeply eclipsing cataclysmic variable containing a magnetic white dwarf primary. The accretion disk is thought to block our line of sight to the white dwarf at all orbital phases due to its extreme inclination angle. Nevertheless, soft X-rays were detected from DQ Her with *ROSAT* PSPC. To probe the origin of these soft X-rays, we have performed *Chandra* ACIS observations. We confirm that DQ Her is an X-ray source. The bulk of the X-rays are from a point-like source and exhibit a shallow partial eclipse. We interpret this as due to scattering of the unseen central X-ray source, probably in an accretion disk wind. At the same time, we detect weak extended X-ray features around DQ Her, which we interpret as an X-ray emitting knot in the nova shell.

Subject headings: Stars: binaries: eclipsing — stars: novae, cataclysmic variables — stars: individual (DQ Her) — X-rays: stars

1. Introduction

A classical nova eruption (see Shara 1989 for a review) is a thermonuclear runaway in a cataclysmic variable (CV; a semi-detached binary in which a white dwarf primary accretes

---

[1]Also Columbia Astrophysics Laboratory, Columbia University, 550 West 120th Street, New York, New York 10027, USA.

[2]Also Universities Space Research Association

from a late-type, usually M dwarf, secondary). The runaway is caused when $\sim 10^{-4}$ M$\odot$ of hydrogen-rich gas is accreted onto the white dwarf surface; this material becomes degenerate, until the pressure and temperature at the base of this envelope starts the runaway reaction. A nova eruption ejects most of the accreted envelope. After a poorly known recurrence time (10^3 – 10^5 years), the underlying binary accumulates enough fresh fuel to erupt again. Novae are of interest to nuclear astrophysicists; they are useful as extragalactic distance indicators; they play a role in Galactic chemical evolution; and they are likely sources of γ-rays. To understand a nova, it is essential to study the underlying system away from its eruption. Conversely, the study of nova eruptions is essential to understand the secular evolution of CVs.

The subject of this paper, DQ Herculis (Nova Herculis 1934), has played a key historical role in the studies of nova eruptions and of post-nova binaries (hereafter old novae) due to its brightness and fortuitous viewing geometry. The 1934 classical nova eruption of DQ Her reached $m_v \sim 1.3$ and enabled extensive observations (see Martin 1989 for a review). The discovery of eclipses in DQ Her (Walker 1956) was pivotal in establishing the standard picture of CVs. Walker (1956) also discovered the coherent 71 sec photometric oscillation: we now understand that DQ Her contains a magnetic white dwarf, accreting onto the magnetic polar regions which are offset from the rotational poles, i.e., an oblique rotator. The ejecta of the 1934 eruption are visible in Hα and other emission lines as an elliptical shell: as of 1978, 43 years after the eruption, the equatorial and polar radii (expansion velocities) of the DQ Her shell were 6.3 ± 0.2 arcsec (384 ± 21 km s^{-1}) and 8.6 ± 0.2 arcsec (528 ± 25 km s^{-1}), respectively (Herbig & Smak 1992). They found no evidence for a deceleration of the expansion, and derived a revised distance estimate of 561±19 pc (we use this value throughout this paper). This makes DQ Her among the nearest old novae known. By 1995 September (61 years after eruption), the equatorial and polar radii have grown to 9.1 ± 0.8 arcsec and 12.5 ± 0.8 arcsec, respectively, still consistent with no deceleration, according to our analysis of an archival *Hubble Space Telescope* WFPC2 image.

The eclipsing nature of DQ Her in principle allows us to place tight constraints on its system parameters. The optical eclipse width, measured from mid-ingress to mid-egress as is customary, is 0.110±0.003 cycles (as compiled from literature by Horne et al. 1993). Assuming that the source of eclipsed light is centered on the white dwarf, this can be used to constrain the relationship between the mass ratio $q = M_2/M_1$ (where M_1 and M_2 denote the masses of the white dwarf and the mass donor, respectively) and the inclination angle i. Horne et al. (1993) measured the radial velocity amplitude of the secondary K_2 through the detection of the Na I infrared doublet absorption lines. This, combined with the eclipse width and the K_1 from literature, have led to their estimates of $q = 0.66 \pm 0.04$, $i = 86°.5 \pm 1°.6$, $M_1 = 0.60 \pm 0.07$ M$_\odot$, and $M_2 = 0.40 \pm 0.05$ M$_\odot$.

About 20 X-ray bright CVs with coherent spin modulations have been discovered since the late 1970s, and are classified as intermediate polars (IPs) or DQ Her stars (Patterson 1994). They are among the brightest CVs in the 2–10 keV band, with luminosities generally in excess of 10^{32} ergs s^{-1}. However, the prototype DQ Her was *not* detected in an *Einstein* Imaging Proportional Counter (IPC) observation with a 2σ upper limit of 0.0046 ct s^{-1} (Córdova et al. 1981). One of their hypotheses, that high inclination may be the cause of this non-detection, found support in a model of the phase shifts of the 71-s oscillation during eclipse (Petterson 1980). In this model, a beam of high energy photons originating on the white dwarf is reprocessed by the accretion disk and results in the optical oscillation. Petterson (1980) finds a good fit at $i \sim 89°$, although the actual value of i can be lower, as long as the entire front half of the disk including the white dwarf is obscured by the outer edge of the disk. Such permanent obscuration of the white dwarf would greatly reduce the X-rays reaching Earth.

Despite the high inclination angle, X-rays were detected from DQ Her with the *ROSAT* Position Sensitive Proportional Counter (PSPC; Silber et al. 1996)[3]. The inferred luminosity (0.1–2.0 keV) of $\sim 4.5 \times 10^{30}$ ergs s^{-1} is modest for an IP. We note that, using a thermal plasma model with $kT = 0.3$ keV with N_H=1.0 $\times 10^{20}$ cm^{-2}, consistent with the PSPC spectrum, and the revised distance of 561 pc (both are different from the values assumed by Córdova et al. 1981), the *Einstein* IPC upper limit corresponds to 2.8 $\times 10^{30}$ ergs s^{-1} in the IPC band (0.4–4 keV), or 3.3 $\times 10^{30}$ ergs s^{-1} in the 0.1–2.0 keV band. These numbers may reflect source variability or the limit of accuracy of cross-instrument comparisons; neither would be surprising. A deep eclipse is not observed, consistent with the permanent obscuration of the white dwarf, suggesting an alternative origin of the observed X-rays. Although Silber et al. (1996) considered a likely origin to be the secondary, it has to be emitting X-rays at significantly above the saturation limit (10^{-3} L_{bol}, or a few times 10^{29} ergs s^{-1} in this case) seen in rapidly rotating late type dwarfs (see, e.g., Singh et al. 1999). If not the secondary, what is the origin of the soft X-rays observed from DQ Her?

Only ~150 photons were detected in the *ROSAT* observation, insufficient for further progress. We have therefore secured a *Chandra* X-ray Observatory Advanced CCD Imaging Spectrometer (ACIS) observation of DQ Her. We describe the observation and data reduction in §2, present the results in §3, and discuss the implications in §4.

---

[3]Patterson (1994) was already aware of this detection, citing "Patterson and Eracleous 1994, in preparation."

2. Observations

We observed DQ Her with *Chandra* (Weisskopf et al. 1996) ACIS without a grating, placing the object on the back-illuminated S3 chip[4]. The observations were performed as two pointings, one from 2001 July 26 13:00 UT to July 27 02:31 UT and the other from 2001 July 29 17:09 UT to July 30 02:27 UT, for a total integration time of 68.8 ksec. These observations were performed at near identical pointing positions and roll angles. We took the outputs from the processing pipeline at the *Chandra* X-ray Center, and extracted images, spectra, and light curves from these observations individually, before combining the results.

DQ Her is clearly detected near the optical position. Even though there is an offset of 1.7 arcsec between the *Chandra* and cataloged positions, somewhat larger the estimated astrometric accuracy of *Chandra* (typically 0.5 arcsec, but up to 1 arcsec; http://cxc.harvard.edu/cal/ASPECT/celmon/), the orbital variability (see §3.2 below) leaves no doubt to the identity of the source.

We extracted source spectra and light curves from a 5 arcsec radius circular region, and background from an annulus of 40 arcsec outer radius and 20 arcsec inner radius centered on the source. The size of the background annulus is chosen to exclude the nova shell emission (see §3.3). The source count rate is 0.025 cts s^{-1} (3 $\times 10^{30}$ ergs s^{-1} in the 0.2–5 keV band, based on the spectral model discussed below), while the background in the source region (scaled from the counts in the background region by the detector areas) is estimated to be 8.2×10^{-4} cts s^{-1}. DQ Her did not show a significant difference in count rate between the two observations.

3. Results

3.1. Spectral Characteristics

We attempted single component fits to the ACIS-S spectrum of DQ Her using power-law, bremsstrahlung, blackbody, and `mekal` (optically-thin thermal plasma emission model; Mewe et al. 1985, 1986; Liedahl et al. 1995) models; none were successful. The simplest successful representation (χ^2_ν=1.3; see Figure 1) is a two-component model consisting of kT=0.63±0.03 keV `mekal` plasma model plus a power law of photon index 1.9±0.2, with N_H = 2.0 ±1.2 × 10^{20} cm^{-2}. Inferred flux in the 0.2–5 keV band is 7.1 $\times10^{-14}$ ergs cm^{-2}s^{-1}, or a luminosity of 2.7 $\times10^{30}$ ergs s^{-1}. DQ Her was not significantly detected above 5.0 keV (we

[4]For details of the ACIS instrument, see the web site at http://www.astro.psu.edu/xray/acis.

obtain a count rate and an estimated 1σ error in the 5–8 keV band of $0.3 \pm 2.0 \times 10^{-4}$ cts s^{-1}), although this is in part due to the lower effective area of the *Chandra* ACIS instrument at high energies. We take 2.0×10^{-4} cts s^{-1} as our upper limit, which corresponds to 4×10^{29} ergs s^{-1} assuming a power law spectral shape with a photon index of 2 and a source distance of 561 pc.

Our adopted model for the spectrum is not unique. There is a bump in the observed spectrum around 1 keV (left panel, Figure 1) which is not in the instrument response. Because of this, the spectrum cannot be fitted with smooth continuum models alone. Using the `mekal` model (right panel, Figure 1), this is interpreted as a complex of lines in the 0.6–1.2 keV range, notably lines of O VIII (0.64 keV), Fe XVII (0.73 & 0.83 keV), and Ne IX (0.90 keV). These lines, however, are weaker relative to the continuum than the predictions of single-temperature plasma models. Moreover, the continuum above 2 keV is much stronger than expected for plasma temperatures that give rise to these lines (kT$\sim$0.6 keV). The power-law component in our model provides the added continuum necessary to achieve an acceptable fit, both near the lines (0.8–1.2 keV) and at higher energies (2–5 keV).

Given the modest number of detected photons ($\sim$1700), and instrumental limitations (both in bandpass and in spectral resolution), there can be a wide range of models that fit the data. We are only confident that DQ Her shows a spectral feature around 1 keV which mimics a collisionally excited, optically-thin plasma of kT$\sim$0.6 keV. Consequently, spectral modeling alone of the *Chandra* data is insufficient to uncover the origin of the soft X-rays in DQ Her.

3.2. Timing Characteristics

We show, in Figure 2, the ACIS light curve of DQ Her folded on the orbital ephemeris of Zhang et al. (1995) into 16 bins per cycle. The ephemeris has an estimated accuracy of $\pm$11 s for this epoch (see §4.1 for further details). A partial eclipse, lasting for about 3 bins and about 30% deep, is clearly seen. In this representation, the X-ray eclipse center appears to be offset from the ephemeris prediction by one half of the binsize, i.e., 0.03 cycle or 500 s. Moreover, the X-ray eclipse appears to be wider (3 bins, or 0.1875 cycles) than the optical eclipse (0.110 ± 0.003, according to a compilation in Horne et al. 1993), which should be 2 bins in Figure 2.

We caution, however, that there is a large uncertainty associated with the X-ray eclipse profile due to the small number of photons. We have experimented with folded light curves using different number of bins per cycle, between 8 and 32. From comparison of 7 different

profiles differing only in bin size, the X-ray eclipse can appear as narrow as 0.13 cycles and the phase offset was as small as 0.025 cycles. Our *Chandra* data are of insufficient quality for us to be able to derive further details of the eclipse profile, such as ingress/egress durations.

3.3. Imaging Characteristics

At first glance, the *Chandra* ACIS image of DQ Her looks like that of a point source. Indeed, over 70% of the flux is contained within 1 arcsec (~560 AU, or 8.4×10^{15} cm) of the image centroid, as expected for a soft point source. However, a closer inspection of the image shows that there is a region about 2 arcsec by 2 arcsec in area and about 10 arcsec NE of the point source with more photons (28) than are expected by chance (~8). These excess counts appear equally distributed over this area, and does not display the sharply peaked core of the point spread function (PSF) expected of a point source.

We have investigated this further by constructing radial profiles of the ACIS image of DQ Her in several energy bands. We then fit a model consisting of a flat background plus the PSF available in the *Chandra* calibration database (interpolated in energy and off-axis angle as appropriate). We find notable excesses in the azimuthally-averaged radial profiles in the 0.2–0.5 and 0.5–0.8 keV bands (Figure 3; we find no significant features at energies above 0.8 keV, although this may in part due to poor counting statistics). The two features marked with horizontal bars (one at 5–9 arcsec in the 0.2–0.5 keV band, and another at 8–10 arcsec in the 0.5–0.8 keV band) appear statistically significant and are likely to be associated with DQ Her. Other possible features either have too few photons (the 6–7 arcsec bin in the 0.5–0.8 keV profile has 5) or outside the optically detected nova shell (12–20 arcsec excess in the 0.2–0.5 keV profile) and will not be discussed further. For the two features, we also construct an azimuthal histogram in 30 degree bins of photons falling within the appropriate radial and energy bins. We plot this in the insets of Figure 3 as a histogram in polar coordinates (the position angle on the graph corresponds to the position angle on the sky, and radial distance from the center is proportional to the number of photons in that bins). We find that the 0.2–0.5 keV feature is about 8 arcsec away S – SW of DQ Her, while the 0.5–0.8 keV feature is about 9 arcsec away NE of the binary.

4. Discussion

4.1. Phase Offset

The folded X-ray light curve appears to be offset from the ephemeris prediction by about 0.03 cycles, or 500 s. The phase offset is likely to be greater than 0.025 cycles. We have carefully checked our data reduction processes and believe this offset to be real.

The linear ephemeris, taken from Zhang et al. (1995), has a nominal error of 11 s for this epoch. Moreover, their linear and quadratic ephemerides have diverged by less than 15 s. Even though a long-term sinusoidal modulation in O−C eclipse timings has been found (Patterson et al. 1978), the magnitude of this effect is 70 s. Thus, we believe that the phase offset likely does not result from an inaccurate ephemeris.

Instead, we consider it likely that the phase shift of the X-ray light curve is caused by departure from axial symmetry of the DQ Her system. We see a considerable scatter in the times of the optical eclipse, up to 170 s in the O−C timings, although some of it can be modeled by the sinusoidal term (see Figure 4 of Zhang et al. 1995). Moreover, the eclipse light curves (see their Figure 1) are obviously skewed, with ingress beginning around phase −0.08 and egress completing around phase +0.12. This clearly demonstrates the departure from axisymmetry of the eclipsed object. We might still argue that the deepest point in the eclipse light curve marks the position of the unseen white dwarf. However, this is not necessarily the case, particularly if the eclipsed object is the back side of an asymmetric accretion disk (Petterson 1980). Interestingly, the radial velocity study of the secondary, using the Na I infrared doublet, shows that the inferior conjunction of the secondary is at phase 0.013±0.009 on the eclipse ephemeris (Horne et al. 1993). This possible phase offset between the radial velocity curve of the secondary and the optical eclipse should be studied further. In any case, a non-axisymmetric disk can result in a phase offset between the optical and X-ray eclipses.

4.2. Eclipse Width

We also have indications that the X-ray eclipse may be wider ($\geq$0.13 cycles, and possibly as wide as 0.19 cycles) than the optical eclipse (0.11 cycles), although this should be confirmed with future observations. Here we consider what these widths mean, and if the apparent difference in X-ray and optical widths might lead to difficulties of interpretation.

The eclipse width is customarily measured from mid-ingress to mid-egress. Since the limb of the secondary passes in front of the center of the white dwarf at mid-ingress and again

at mid-egress (ignoring the curvature of the secondary), this definition of the width leads to a unique constraint on the q - i relationship, regardless of the size of the eclipsed object. This is done by comparing the measured width with that calculated for the white dwarf center using the full Roche potential, as detailed by Bailey (1979). The key assumption in this procedure is that the source of eclipsed light is centered on the white dwarf. This assumption may not hold for the optical light in DQ Her, and almost certainly does not hold for its X-rays.

Recall the model of Petterson (1980) for the phase shift of the 71-s oscillations. A good fit was obtained if the front half of the accretion disk is obscured by its outer edge. This implies that the emission-weighted center of eclipsed light is somewhere on the back half of the accretion disk, further away from the secondary than the white dwarf. If true, the inclination angle i derived with the usual assumption, as Horne et al. (1993) have adopted, would be an underestimate for a given q. We cannot solve this difficulty with the data in hand, so we treat this as an extra source of uncertainty in the analysis to follow.

4.3. Wind-Scattered X-rays

At this inclination, a partial eclipse is a signature of an extended emission region. Any X-ray emission or scattering from the surface of the accretion disk should be as deeply eclipsed as the optical light from the disk. Since the X-ray eclipse is much shallower than in the optical, we conclude that the X-rays must originate in a vertically extended region. Assuming the best-fit system parameters of Horne et al. (1993), we estimate that materials that are $> 0.28a$ (where a is the binary separation) above the orbital plane should remain uneclipsed. The limit could be somewhat larger if the inclination is underestimated by Horne et al. (1993).

Is this a single, extended X-ray source, or can there be an eclipsed component and an uneclipsed component? From the data in hand, we cannot rule out the latter possibility. We could test this if we had a higher quality X-ray light curve of the eclipse. A two-component model would predict a sharp ingress and egress, while a single extended source would result in a more gradual eclipse transitions. Here we proceed assuming a single extended source, since we do not have a physical model corresponding to the two-component model.

An extended X-ray source in DQ Her, high above the orbital plane, is consistent with the idea that the observed X-rays have been reprocessed in the accretion disk wind. This situation is similar to those of two non-magnetic CVs, the dwarf nova OY Car in superoutburst (Naylor et al. 1988; Pratt et al. 1999) and in the nova-like variable UX UMa (Wood

et al. 1995). Both are deeply eclipsing systems in the optical, yet no X-ray eclipses were observed by these authors. Their interpretation is a central X-ray source which cannot be directly seen, but is indirectly seen after scattering in an extended corona or wind. The *EUVE* observation of OY Car in superoutburst (Mauche & Raymond 2001) confirms this basic picture, since the observed spectrum can be modeled as resonant scattering of continuum photons in an accretion disk wind. A wind, rather than a static corona, is strongly favored since the EUV emission lines are seen to have FWHM of $\sim$2300 km s^{-1}. We believe this is also the likely interpretation for DQ Her.

Among CVs, it is usually the non-magnetic systems with high accretion rate that have an accretion disk wind (see, e.g., Drew & Proga 2000). Both OY Car in superoutburst and UX UMa are good examples. These systems have an accretion disk that extends all the way down to the white dwarf surface and an optically thick boundary layer. The latter is believed to be the source of strong soft X-rays and modest hard X-rays seen in non-eclipsing systems, and probably helps drive the wind. This is not the case with DQ Her: the disk is believed to be truncated by the primary's magnetic field, with subsequent accretion taking place along the primary's field lines. Nevertheless, DQ Her has UV emission lines that are only partially eclipsed, which is strong evidence for the presence of an accretion disk wind in this magnetic CV (Córdova & Mason 1985; Silber et al. 1996; Eracleous et al. 1998).

A static corona can also be the scattering site for the X-ray photons observed in DQ Her. However, that would make it different from OY Car, where the EUV line widths prove the wind to be responsible for scattering. Secondly, we know that a wind exists in DQ Her, while we don't know if a corona exists in this system. Finally, the depth of the partial eclipse demands a large vertical extent ($> 0.28a$, see above) for the scattering region. This is well away from the disk and probably is an unlikely location for a static corona.

We therefore conclude that resonant scattering in the wind is the likely source of observed X-rays, pending final confirmation in the form of X-ray line widths. It is interesting to note that a partial X-ray eclipse is detected in DQ Her, while none has been found in OY Car or UX UMa. It is not clear, however, whether this indicates some difference in the wind between magnetic and non-magnetic systems, or if this is simply due to the more extreme inclination angle in DQ Her.

4.4. Non-Detection of Reflected X-rays

The observed X-ray luminosity of 3–5 $\times 10^{30}$ ergs s^{-1} is likely to be a small fraction of the intrinsic luminosity of the central source, although this depends strongly on the unknown

efficiency of scattering in the wind. The flux of the He II λ1640 line has been used to estimate an ionizing luminosity of 1–2 $\times 10^{34}$ ergs s^{-1} (Silber et al. 1996; Eracleous et al. 1998).

Can this be in the form of a hard component (kT$\sim$20 keV bremsstrahlung) usually seen in IPs? To investigate this question, we have modeled the reflection of such a component off the surface of the Roche-lobe filling secondary, applying the method of Still et al. (2001) developed for Hercules X-1. X-rays hitting the cold material on the surface of the secondary can be scattered or absorbed; since softer photons are more likely to be absorbed, the scattered component is harder than the incident component. We have evaluated the 5–8 keV flux expected from reflection from the secondary as a function of the orbital phase, taking into account the shadowing by the accretion disk and the Roche-lobe filling shape of the secondary, assuming the system parameters of Horne et al. (1993), as listed in §1. For the computational details, see Still et al. (2001).

The reflection component should be most prominent at the highest energy band of *Chandra*, 5–8 keV. The viewing geometry for the reflection component is most favorable at orbital phase 0.5; it would result in a strong, sinusoidal orbital modulation. However, no such component is detected in our *Chandra* data in the 5–8 keV data. This can be converted to the upper limit of the bolometric luminosity of the hard component as a function of the disk thickness (Figure 4). Taking our upper limit in the phase bin around phase 0.5, 1/16th cycle wide, to be 7.0×10^{-4} cts s^{-1}, we estimate an upper limit to the kT=20 keV bremsstrahlung luminosity of 10^{33} ergs s^{-1} for a disk H/R (height over radius) of less than 0.23, or half-opening angle $< 13°.0$ ($< 14°.6$ for a kT=50 keV bremsstrahlung due to the different bolometric correction). If the intrinsic hard component luminosity is 10^{34} ergs s^{-1}, the reflected luminosity can be reduced to an undetectable level if the disk half opening angle is $> 17°.7$ for kT=20 keV ($> 18°.0$ for kT=50 keV), almost completely shadowing the secondary.

In comparison, the eclipsing and dipping low-mass X-ray binary EXO 0748−676 has an inclination of $i \sim 75°$ (Parmar et al. 1986): The presence of X-ray eclipse requires the opening angle of the disk to be less than 15° toward the secondary in this system. Although azimuthal structures at such heights are commonly inferred (including one in U Gem 25° above the disk; Szkody et al. 1996), we are not aware of claims for disks thicker than 15° in the direction toward the secondary. We therefore conclude that the central hard X-ray component is less luminous than inferred from the He II λ1640 line, unless the disk in DQ Her has an unusually large thickness. Further studies of the disk thickness, however, are required to tighten the upper limit of the hard component luminosity.

In contrast, the lack of reflection component does not allow us to put a useful constraint on the central luminosity, if it has a soft spectrum. Accretion luminosity in DQ Her would

be dominated by a soft, blackbody-like component, if the shock is buried within the white dwarf atmosphere. In addition, the entire photosphere of the primary may still be hot from the thermonuclear runaway of 1934. The soft component in AM Her type magnetic CVs have a typical temperature of 20–30 eV (Mauche 1999); even using a kT=100 eV blackbody, the spectrum is too soft to result in appreciable reflection signature. Therefore, our results are consistent with the ionizing luminosity of 1–2 $\times 10^{34}$ ergs s^{-1} (Silber et al. 1996; Eracleous et al. 1998) if this is in the form of a soft component, regardless of the disk height.

4.5. The Nova Shell around DQ Her

We have detected extended emission features, one about 8 arcsec S to SW of, and another about 9 NE of DQ Her. The latter location corresponds to a bright [N II] knot in the DQ Her shell, while the former has no obvious optical feature associated with it (Slavin et al. 1995). We consider it likely that these small excesses are X-ray knots in the DQ Her shell. A similar, but much brighter, X-ray shell has been seen around GK Per (Nova Persei 1901; Balman & Ögelman 1999). This shell has a soft thermal spectrum, with a prominent Ne IX line at 0.9 keV (Balman 2002). We do not have enough photons for a spectral analysis for the DQ Her shell, but it appears much softer than the GK Per shell. This could result from a different speed class (DQ Her was a slow nova, while GK Per was a fast nova), as well as from a different environment around DQ Her than around GK Per. The luminosity in the DQ Her knot appears to be a few times 10^{28} ergs s^{-1}, subject to a large uncertainty in count rate to flux conversion, due to the unknown spectral shape.

Given the probable discovery of X-rays from the shell, and the apparent lack of strong hard X-rays from the central source, it may be useful to revisit the models of UV and optical spectra of the shell. For example, Ferland & Truran (1981) assumed a hard X-ray emitting magnetic CV with a luminosity in excess of 10^{34} ergs s^{-1} as the source of ionizing photons. Our work casts some doubt on such a picture. Petitjean et al. (1990), on the other hand, assumed a 10^5 K blackbody source, which is consistent with our X-ray data of the central binary. However, how do the shell X-rays fit in?

Balman (2002) interprets the X-rays from the GK Per shell as a miniature supernova remnant. In this model, the nova ejecta are plowing into the surrounding interstellar medium and shock heated into X-ray emitting temperatures. There certainly is ample kinetic energy in the nova ejecta to power shell X-ray emission, and the ejecta velocities are fast enough to result in X-ray emitting temperatures. The photoionization model of UV and optical lines, on the other hand, suggest a cold shell. We regard this not as an outright contradiction, but as an additional evidence for the co-existence of hot and cold matter in nova shells. We

have long known of spectra that show both hot and cold components in nova shells (Payne-Gaposchkin 1957; Williams 1992). More recent imaging results (Slavin et al. 1995) and theoretical works (Lloyd et al. 1997) show the importance of Rayleigh-Taylor instability. Nova shells are complex, multi-phased entities, including, as it now appears, X-ray emitting knots.

5. Conclusions

Our *Chandra* observation of the old nova DQ Her have revealed a partial X-ray eclipse. We believe that the most likely explanation is scattering in the accretion disk wind, with a central X-ray source which is hidden from our view by the accretion disk at all orbital phases. In this model, DQ Her is similar to OY Car in superoutburst and to UX UMa. With a higher signal-to-noise observation, such as we can hope to achieve with *XMM-Newton*, we should be able to measure the X-ray eclipse profile in detail, and check the reality of the phase offset between X-ray and optical eclipses.

We also detect a weak extended feature, which we believe is an X-ray emitting knot in the nova shell. Thus DQ Her joins GK Per as classical novae with an X-ray emitting shell. Although an *XMM-Newton* observation will collect more photons, its spatial resolution may not be sufficient to study the weak extended emission within 10 arcsec of a much brighter point source.

REFERENCES

Bailey, J. 1979, MNRAS, 187, 645

Balman, S. & Ögelman, H.B. 1999, ApJ, 518, L111

Balman, S. 2002, in "High Energy Universe at Sharp Focus," eds. E.M. Schlegel & S.D. Vrtilek, ASP Conf. Ser., 262, 34

Córdova, F.A. & Mason, K.O. 1985, ApJ, 290, 671

Córdova, F.A., Mason, K.O. & Nelson, J.E. 1981, ApJ, 245, 609

Drew, J.E. & Proga, D. 2000, New Astron. Rev. 44, 21

Eracleous, M., Livio, M., Williams, R.E., Horne, K., Patterson, J., Martell, P. & Korista, K.T. 1998, in "Wild Stars in the Old West," eds. S. Howell, E. Kuulkers & C. Woodward, ASP Conf. Ser., 137, 438

Ferland, G.J. & Truran, J.W. 1981, ApJ, 244, 102

Herbig, G.H., & Smak, J.I. 1992, Acta Astron., 42, 17

Horne, K., Welsh, W.F. & Wade, R.A. 1993, ApJ, 410, 357

Liedahl, D.A., Osterheld, A.L. & Goldstein, W.H. 1995, ApJ, 438, 115

Lloyd, H.M., O'Brien, T.J. & Bode, M.F. 1997, MNRAS, 286, 137

Martin, P.G. 1989, Classical Novae, M.F. Bode & A. Evans, J. Wiley & Sons, 1989, p. 93

Mauche, C.W. 1999, in "Annapolis Workshop on Magnetic Cataclysmic Variables," eds. by C. Hellier & K. Mukai, ASP Conf. Ser., 157, 157

Mauche, C.W. & Raymond, J.C. 2001, ApJ, 541, 924

Mewe, R., Gronenschild, E.H.B.M. & van den Oord, G.H.J. 1985, A&AS, 62, 197

Mewe, R., Lemen, J.R. & van den Oord, G.H.J. 1986, A&AS, 65, 511.

Naylor, T., Bath, G.T., Charles, P.A., Hassall, B.J.M., Sonneborn, G., van der Woerd, H. & van Paradijs, J. 1988, MNRAS, 231, 237

Parmar, A.N., White, N.E., Giommi, P. & Gottwald, M. 1986, ApJ, 308, 199

Patterson, J. 1994, PASP, 106, 209

Patterson, J., Robinson, E.L. & Nather, R.E. 1978, ApJ, 224, 570

Payne-Gaposchkin, C. 1957, The Galactic Novae, North Holland, Amsterdam

Petitjean, P., Boisson, C. & Péquignot, D. 1990, A&A, 240, 433

Petterson, J.A. 1980, ApJ, 241, 247

Pratt, G.W., Hassall, B.J M., Naylor, T., Wood, J.H. & Patterson, J. 1999, MNRAS, 309, 847

Shara, M. 1989, PASP, 101, 5

Silber, A.D., Anderson, S.F., Margon, B. & Downes, R.A. 1996, ApJ, 462, 428

Singh, K.P, Drake, S.A., Gotthelf, E.V. & White, N.E. 1999, ApJ, 512, 874

Slavin, A.J., O'Brien, T.J. & Dunlop, J.S. 1995, MNRAS, 276, 353

Still, M., O'Brien, K., Horne, K., Boroson, B., Titarchuk, L.V., Engle, K., Vrtilek, S.D., Quaintrell, H. & Fieldler, H. 2001, ApJ, 554, 352

Szkody, P., Long, K.S., Sion, E.M. & Raymond, J.C. 1996, ApJ, 469, 834

Walker, M.F. 1956, ApJ, 123, 68

Weisskopf, M. C., O'Dell, S. L., & van Speybroeck, L. P. 1996, Proc. SPIE, 2805, 2

Williams, R.E. 1992, AJ, 104, 725

Wood, J.H., Naylor, T. & Marsh, T.R. 1995, MNRAS, 274, 31

Zhang, E., Robinson, E.L., Stiening, R.F. & Horne, K. 1995, ApJ, 454, 447

This preprint was prepared with the AAS LaTeX macros v5.0.

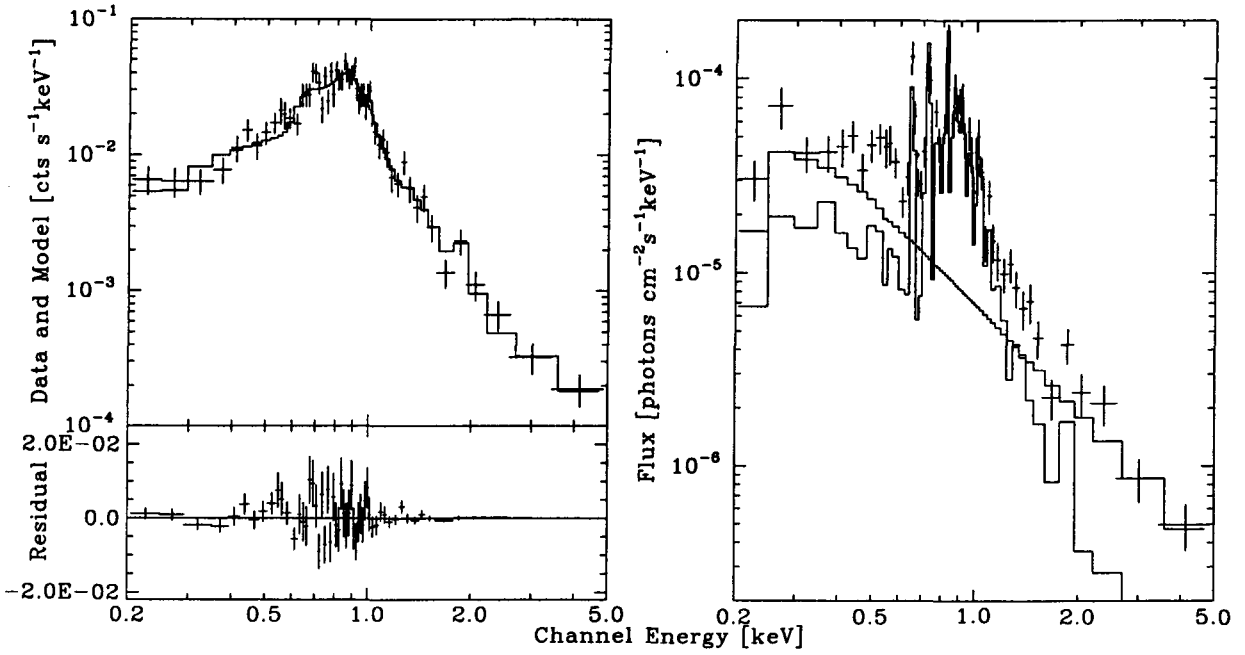

Fig. 1.— The *Chandra* ACIS spectrum of DQ Her: (left) The observed spectrum is shown in upper panel, with the best-fit two component model folded through the instrument response, while the residuals are shown in the lower panel; (right) The photon spectrum inferred from the fit, shown with the power-law and thin thermal plasma components.

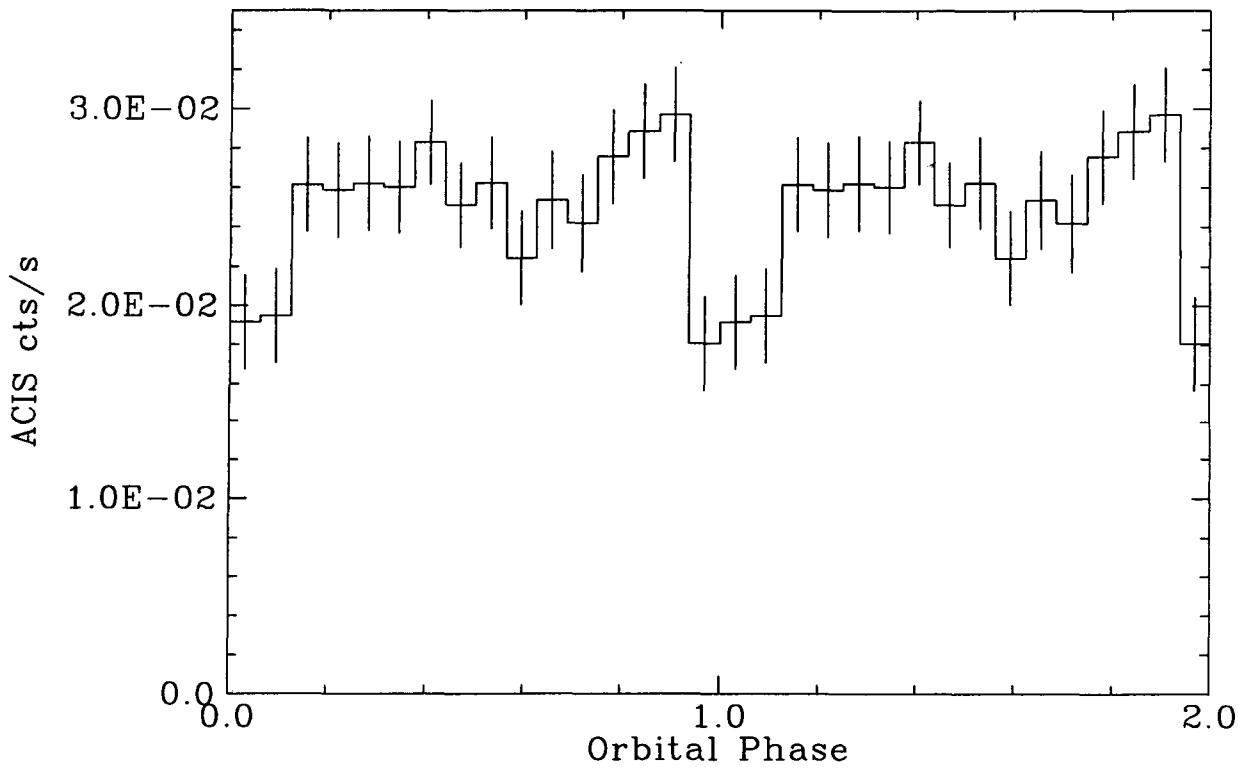

Fig. 2.— The *Chandra* ACIS light curve of DQ Her, folded on the orbital period and plotted twice. Each bin is 1/16th of the orbital period.

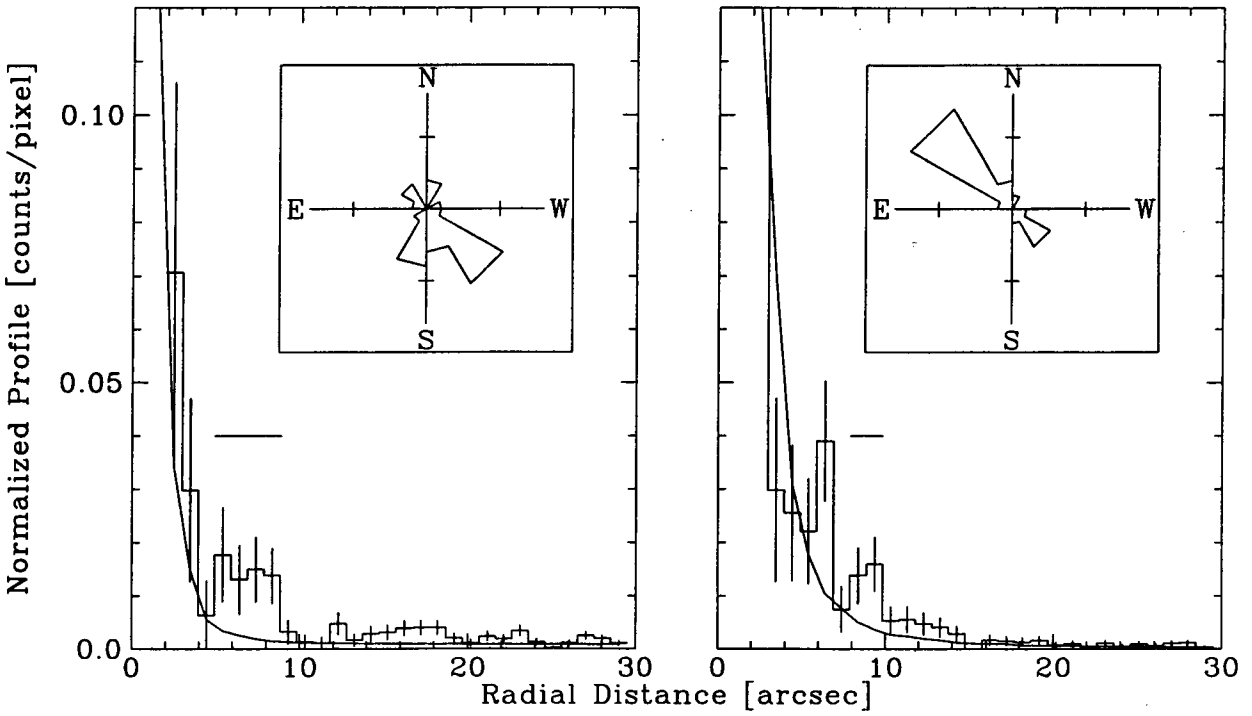

Fig. 3.— The radial profiles of the *Chandra* ACIS-S X-ray image of DQ Her in the 0.2–0.5 keV (left) and 0.5–0.8 keV (right) bands. The data are plotted as a histogram with errors, while the best-fit model are plotted as a solid line. The central ∼1 arcsec determines the normalization of the profile, but has been omitted from this figure to make the wings of the PSF visible. The horizontal bars indicate the two prominent features examined further in the insets. They are histograms in polar coordinates of the excess counts (see text for details). Tick marks indicate 5 counts per bin.

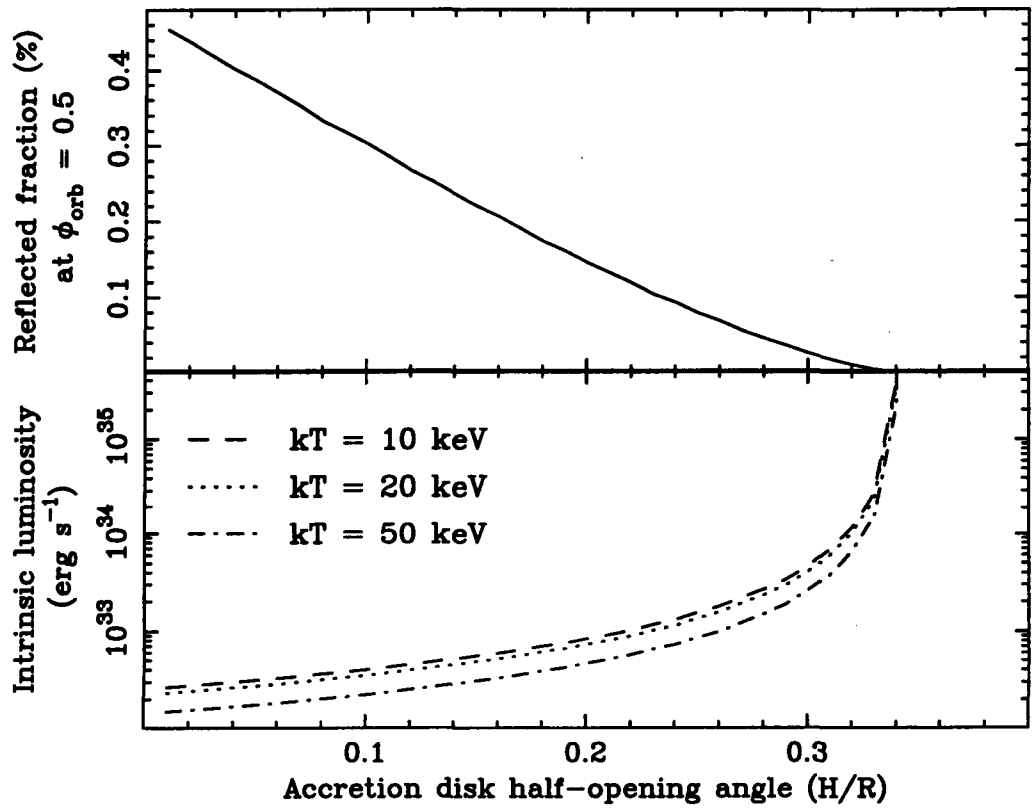

Fig. 4.— (Top) The calculated efficiency of reflection from the secondary star at orbital phase 0.5. The reflection fraction in the 5–8 keV band is plotted as a function of the thickness of the accretion disk. (Bottom): The inferred upper limit to the central hard component for three different bremsstrahlung temperatures, as a function of the disk thickness.